

# Long fiber Bragg grating sensor interrogation using discrete-time microwave photonic filtering techniques

Amelia Lavinia Ricchiuti,<sup>1,\*</sup> David Barrera,<sup>1</sup> Salvador Sales,<sup>1</sup> Luc Thévenaz,<sup>2</sup>  
and José Capmany<sup>1</sup>

<sup>1</sup>*IITEAM Research Institute, Universidad Politécnica de Valencia, Camino de Vera s/n, 46022 Valencia, Spain*

<sup>2</sup>*Ecole Polytechnique Fédérale de Lausanne, Institute of Electrical Engineering, SCI-STI-LT Station 11, 1015 Lausanne, Switzerland*

\**amric1@iteam.upv.es*

**Abstract:** A novel technique for interrogating photonic sensors based on long fiber Bragg gratings (FBGs) is presented and experimentally demonstrated, dedicated to detect the presence and the precise location of several spot events. The principle of operation is based on a technique used to analyze microwave photonics (MWP) filters. The long FBGs are used as quasi-distributed sensors. Several hot-spots can be detected along the FBG with a spatial accuracy under 0.5 mm using a modulator and a photo-detector (PD) with a modest bandwidth of less than 1 GHz. The proposed interrogation system is intrinsically robust against environmental changes.

©2013 Optical Society of America

**OCIS codes:** (060.3735) Fiber Bragg gratings; (060.2370) Fiber optics sensors; (230.1480) Bragg reflectors.

---

## References and links

1. B. Culshaw, "Optical fiber sensor technologies: opportunities and perhaps pitfalls," *J. Lightwave Technol.* **22**(1), 39–50 (2004).
2. A. D. Kersey, M. A. Davis, H. J. Patrick, M. LeBlanc, K. P. Koo, C. G. Askins, M. A. Putnam, and E. J. Friebele, "Fiber grating sensors," *J. Lightwave Technol.* **15**(8), 1442–1463 (1997).
3. S. Y. Li, N. Q. Ngo, S. C. Tjin, P. Shum, and J. Zhang, "Thermally tunable narrow-bandpass filter based on a linearly chirped fiber Bragg grating," *Opt. Lett.* **29**(1), 29–31 (2004).
4. H. Uno, A. Kojima, A. Shibano, and O. Mikami, "Optical wavelength switch using strain-controlled fiber Bragg gratings," *Proc. SPIE* **3740**, 274–277 (1999).
5. J. Azaña and M. A. Muriel, "Temporal self-imaging effects: theory and application for multiplying pulse repetition rates," *IEEE J. Sel. Top. Quantum Electron.* **7**(4), 728–744 (2001).
6. M. Volanthen, H. Geiger, and J. P. Dakin, "Distributed grating sensors using low-coherence reflectometry," *J. Lightwave Technol.* **15**(11), 2076–2082 (1997).
7. H. Murayama, H. Igawa, K. Kageyama, K. Ohta, I. Ohsawa, K. Uzawa, M. Kanai, T. Kasai, and I. Yamaguchi, "Distributed strain measurement with high spatial resolution using fiber Bragg gratings and optical frequency domain reflectometry," in *Optical Fiber Sensors*, OSA Technical Digest (CD) (Optical Society of America, 2006), paper ThE40.
8. K. Hotate and K. Kajiwar, "Proposal and experimental verification of Bragg wavelength distribution measurement within a long-length FBG by synthesis of optical coherence function," *Opt. Express* **16**(11), 7881–7887 (2008).
9. J. Sancho, S. Chin, D. Barrera, S. Sales, and L. Thévenaz, "Time-frequency analysis of long fiber Bragg gratings with low reflectivity," *Opt. Express* **21**(6), 7171–7179 (2013).
10. J. Capmany, B. Ortega, D. Pastor, and S. Sales, "Discrete-time optical processing of microwave signals," *J. Lightwave Technol.* **23**(2), 702–723 (2005).
11. J. Capmany, J. Mora, I. Gasulla, J. Sancho, J. Lloret, and S. Sales, "Microwave photonic signal processing," *J. Lightwave Technol.* **31**(4), 571–586 (2013).
12. L. R. Chen, S. D. Benjamin, P. W. E. Smith, and J. E. Sipe, "Ultrashort pulse reflection from fiber gratings: a numerical investigation," *J. Lightwave Technol.* **15**(8), 1503–1512 (1997).
13. B. E. A. Saleh and M. C. Teich, *Fundamentals of Photonics*, 2nd ed. (Wiley, New York, 2007).

---

## 1. Introduction

FBGs have established their role as key devices in fiber optic-based signal processing systems and applications due to their advantageous characteristics such as simplicity, low insertion

loss, polarization independence, low cost and seamless integration in fiber optics systems. Furthermore, FBGs are made of dielectric material and hence non conducting, immune to electromagnetic interference (EMI), chemically inert and spark free [1]. For these reasons, FBGs have been extensively implemented in different kinds of application scenarios such as sensors [2], filters [3], switches [4] and for multiplying pulse repetition rates [5], amongst others. In the context of sensing applications, different methods have been proposed and implemented in order to interrogate the Bragg-frequency distribution along a FBG with the aim of implementing distributed temperature/strain sensors. Some of these salient techniques include optical low-coherence reflectometry (OLCR) [6], optical frequency domain reflectometry (OFDR) [7], synthesis of optical coherence function (SOCF) [8], and time-frequency analysis [9].

In this work, a novel technique to interrogate long FBGs and its potential applications to fiber sensing is proposed and demonstrated. This technique brings several advantages derived from the fact that it relies on interference in the microwave rather than optical domain. Microwave interferometry is by far more stable and easier to control and, if suitably combined with photonics, provides a remarkable spatial accuracy. Furthermore, the system spectral performance can be easily reconfigured, since the sensor is based on a discrete time filter configuration. The proposed system is specifically dedicated to the situation where one or more spot events must be precisely identified and located, such as hot-spots or cracks in structures. The fundamental concept for the proposed interrogation technique is inspired on the operation principle of a discrete time Microwave Photonic (MWP) filter [10, 11], in particular on the information on the delays between the different taps of the filter provided by measuring its radiofrequency transfer function given by the  $S_{21}$  parameter. The hot-spot position can be evaluated with a spatial accuracy under 0.5 mm. In the simple configuration proposed, the objective has not been the evaluation of the exact value of temperature or strain, but the detection of its presence and position. However, by opportunely controlling the tunable bandpass filter of our system, it is certainly able to provide an estimation of the magnitude under measurement, without using any more devices or additional wavelength-scanned systems. To demonstrate the performance of the proposed technique, firstly, a 10-cm long strong FBG has been fabricated as a sensing device able to detect one or more hot-spots having different temperatures and located at certain points of the grating. Then, in order to reduce the bandwidth of the devices used in the interrogation system (modulator and photo-detector), a reference arm has been included achieving a correct performance of the quasi-distributed sensor operating with a modest bandwidth of only 1 GHz.

## 2. Principle of operation

The setup used to interrogate the long FBG is based on the principle of operation of a MWP filter and is depicted in Fig. 1. The output of a continuous wave (CW) light source is electro-optically modulated with a microwave signal. At the output of the electro-optical modulator (EOM) the modulated optical signal is split into  $N$  arms. Each arm has a delay-line and an attenuator (or amplifier) in order to provide a delayed and weighted replica of the original signal. These time-delayed and weighted optical signals are combined together and photo-detected. In the detection process, the different taps can be mixed according to either a coherent or an incoherent basis. In case of incoherent mixing, the tap combination at the photo-detector (PD) is insensitive to environmental effects, stable and with a remarkably good repeatable performance. For these reasons, the experimental setup that it is proposed to interrogate the long FBG has been implemented under incoherent operation. The microwave signal is acquired and the electrical frequency response  $H(\omega)$  of such a structure is given by [11]:

$$H(\omega) = \sum_{k=0}^N a_k e^{-ik\omega T_k}. \quad (1)$$

where  $\omega$  is the microwave frequency and  $a_k$  is the weight of the  $k$ -th replica that is delayed by  $T_k$ . When  $T_k = T, \forall k$  Eq. (1) identifies a transfer function with a periodic spectral characteristic; the frequency period is known as *free spectral range* (FSR) and it is inversely proportional to the spacing  $T$  between samples [11].

The proposed sensor produces delayed replicas of the original signal at the input end of the FBG and at each of the hot-spots to be measured [9, 12]. Thus, the response of the FBG sensor is described also by Eq. (1), where the number of taps is equal to the number of hot-spots plus one – the reference reflection normally placed at the entry point of the FBG – and the delays are given by the product of the speed of light within the FBG and the distance between the beginning of the FBG and the location of each hot-spot (see Fig. 1).

The main limitation of this technique arises from the fact that the conditions for incoherent regime operation have to be guaranteed. This implies that the minimum delay between two consecutive hot-spots,  $T = \min\{T_{k+1} - T_k\}$  has to verify that  $t_c \ll T$  where  $t_c$ , the optical source coherence time is given by [13]:

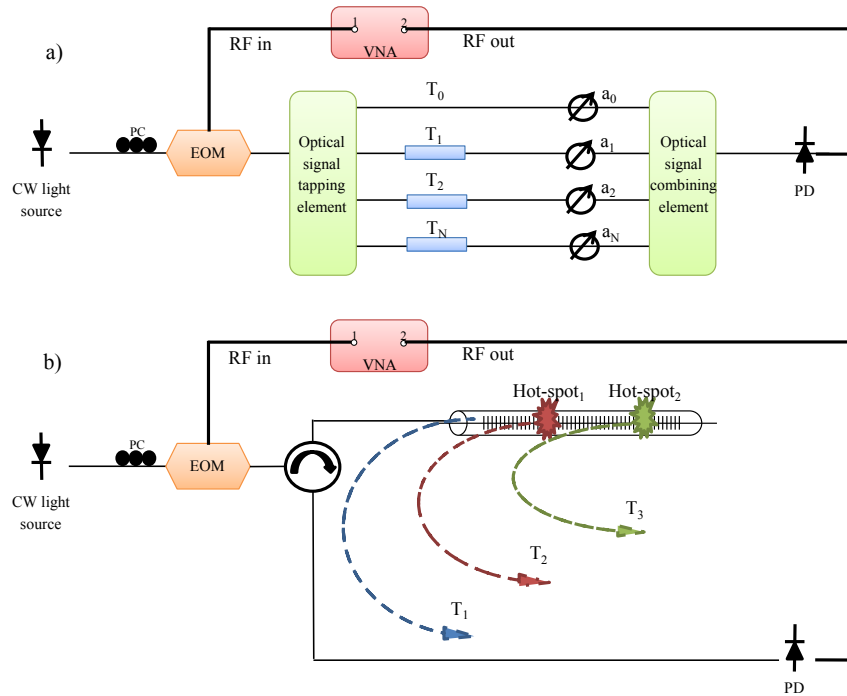


Fig. 1. a) Schematic diagram of an  $N$  tap microwave photonic filter. b) Schematic diagram of the interrogation of the long FBG using microwave photonic techniques.

$$t_c = \frac{1}{\Delta f}. \quad (2)$$

Here  $\Delta f$  is the typical spectral bandwidth of the source. To reduce the value of  $t_c$  and to obtain a better range, a broadband source is proposed. The delay between the two consecutive hot-spots is related to the distance  $L$  between them by:

$$T = \frac{2n_o L}{c}. \quad (3)$$

where  $n_o$  is the refractive index of the fiber and  $c$  is the speed of light in vacuum. Therefore, to secure an incoherent regime:

$$L \gg \frac{c}{2n_o \Delta f} = \frac{\lambda^2}{2n_o \Delta \lambda}. \quad (4)$$

where  $\Delta f = c\Delta\lambda/\lambda^2$  being  $\Delta\lambda$  the source linewidth in wavelength units and  $\lambda$  the central emission wavelength.

### 3. Setup and experimental measurements

Figure 2 shows the experimental setup used to interrogate a 10-cm long FBG with  $\approx 99\%$  reflectivity and  $\approx 14$  GHz FWHM. A broadband signal provided by a semiconductor optical amplifier (SOA) is filtered by means of a tunable bandpass filter featuring a bandwidth of 0.45 nm centered at the Bragg wavelength of a long FBG. The resonance of the FBG is 1554 nm at room temperature. Using Eq. (2), a time coherence of 17.78 ps for the filtered optical source is obtained, which dictates smallest time spacing between hot-spots of  $\sim 100$  ps. This implies that the distance between hot-spots should be longer than 10 mm to maintain the conditions of the incoherent regime.

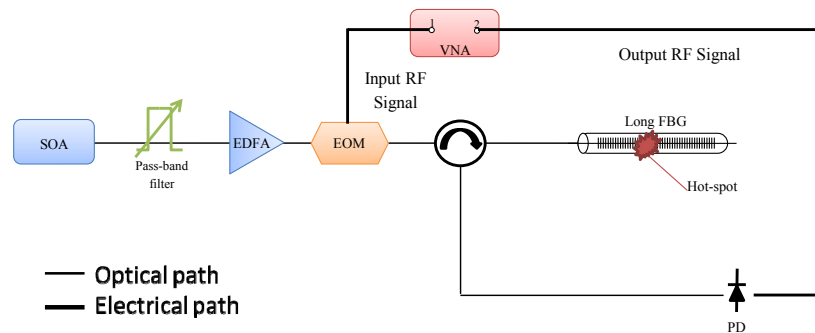


Fig. 2. Experimental setup used to interrogate the 10-cm long strong FBG.

The output of the tunable filter is electro-optically modulated with a microwave signal generated by a Vector Network Analyzer (VNA). The microwave signal consists of a radio frequency (RF) tone swept from 10 MHz to 10 GHz. At the output of the EOM, the signal is sent into the FBG through an optical circulator. The signal reflected by the grating is photo-detected. In this way, the frequency response of the system can be analyzed by monitoring the scattering parameter  $S_{21}$ , which relates the RF detected signal to the input modulating microwave signal.

Due to the high reflectivity of the FBG, most of the input signal is reflected at the initial section of the FBG [12]. However, a local change of temperature in a 5 mm hot-spot placed at a certain point along the grating will produce a local Bragg frequency shift. When this occurs, besides the main reflected signal, which is generated at the initial section of the grating, a second reflected signal is produced at the point where the hot-spot is placed. In this way, the presence of a hot-spot results in a two tap MWP filter and it is possible to determine the location of the hot-spot zone by evaluating the FSR of the filter as it is described by Eq. (1).

Figure 3(a) shows the experimental results obtained by moving the hot-spot along the FBG while the inset shows the hot-spot position. As expected the recovered response is similar to a two tap MWP filter. The FSR has been evaluated with a frequency step of 0.01 MHz, which corresponds to an estimated spatial accuracy under 0.5 mm. The length spacing between the two taps is calculated according to the Eq. (3) and from this value the hot-spot position is determined. Figure 3(b) illustrated a comparison between the hot-spot position calculated from the Inverse Fourier Transform (IFT) of the amplitude of the filter transfer function (dots) and the theoretical inverse linear relation (solid line).

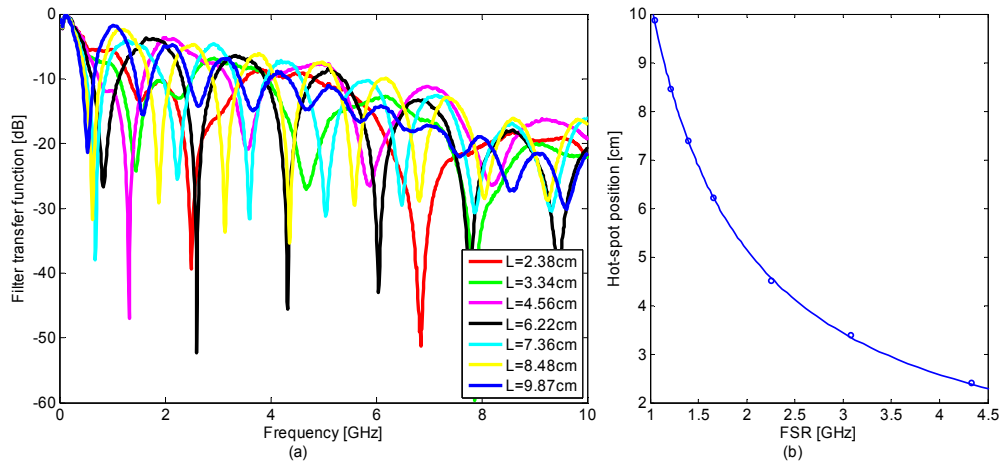


Fig. 3. a) Frequency response of the two tap filters achieved by placing a hot-spot on the FBG. Inset: Hot-spot position. Fig. 3. b) Comparison between the hot-spot position calculated from the IFT (dots) and the theoretical inverse linear relation (solid line).

Figure 4(a) shows the response of the sensor when one and two hot-spots are present (two and three tap filter, correspondingly). Since retrieving the delays directly from the transfer function is time consuming, the most efficient approach to calculate the distance between the input end of the FBG and the two hot-spots is simply to take the IFT of the measured  $S_{21}$  parameter. Figure 4(b) shows the IFT of the amplitude of the three tap filter transfer function illustrated in Fig. 4(a) where two hot-spots are placed along the grating and the IFT of the amplitude of the two tap filter obtained when one of the hot-spots is suppressed.

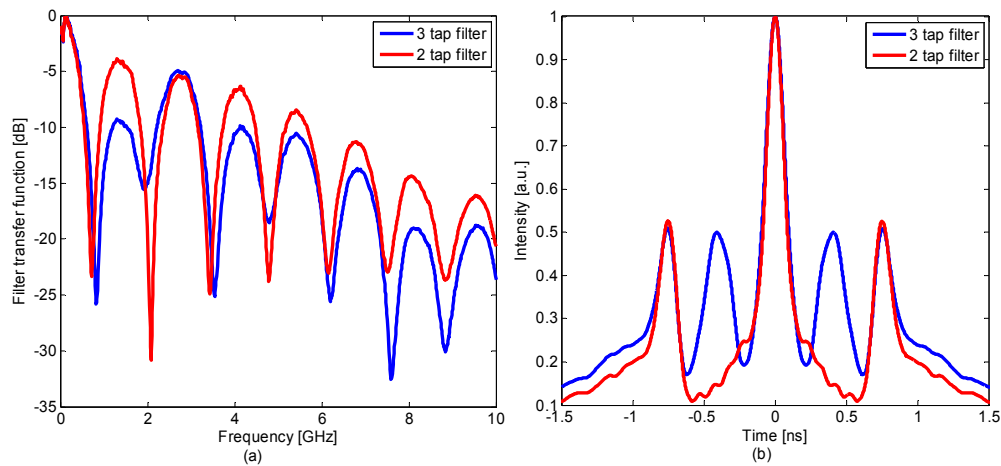


Fig. 4. a) Frequency response of three tap and two tap filters obtained by placing two hot-spots and one hot-spot along the grating, respectively. Fig. 4. b) Inverse Fourier transforms of the amplitude of the MWP filters shown in Fig. 4(a).

The time differences between the main peaks and the two pairs of sub-pulses from Fig. 4(b) (blue curve) represent the time spacing  $T_1$  and  $T_2$  between the beginning of the FBG and the first and second hot-spot, respectively. By using Eq. (3), the distance between the entry point of the grating and the first hot-spot is calculated to be 4.20 cm, while the distance between the grating entry point and the second hot-spot is 7.82 cm.

To alleviate the bandwidth requirements of the modulator and the PD, a variant of the setup is proposed, which is illustrated in Fig. 5. A reference arm is used in this case in order to

obtain higher time spacing  $T$  between taps, which leads to a shorter FSR, when only one hot-spot is detected. In this case, the hot-spot position can be evaluated by using a modulator and a PD with a modest bandwidth of less than 1 GHz.

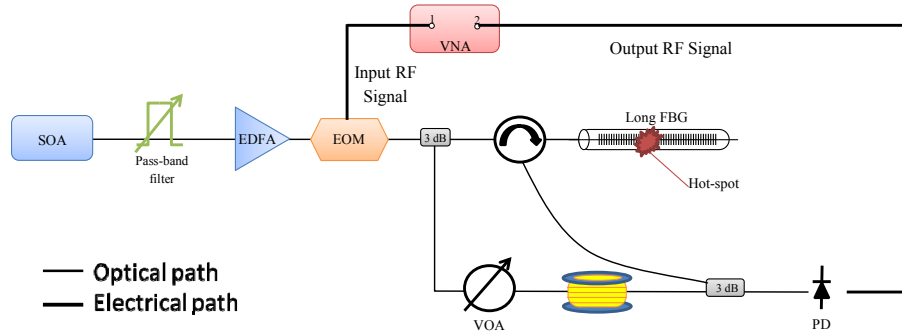


Fig. 5. Experimental setup using a reference arm to obtain higher time spacing between taps.

The blue curve in Fig. 6(a) and Fig. 6(b) represents the two tap filter created by the combination of the tap provided by the signal reflected by the FBG and the tap provided by the reference arm. When a hot-spot is placed along the FBG, another tap is created, actually resulting in a three tap MWP filter. But, a two tap filter is desirable to simplify the measurement process; for this reason, by judiciously tuning the optical bandpass filter, the tap created at the initial section of the FBG is filtered out and a two tap MWP filter is actually obtained - due to the combination of the tap provided by the signal reflected by the hot-spot and the tap provided by the reference arm. Figure 6(c) illustrated a comparison between the hot-spot position calculated from the IFT (dots) and the theoretical inverse linear relation (solid line). Once again the location of the hot-spot in the FBG can be calculated using Eq. (3) with a spatial accuracy of less than 0.5 mm.

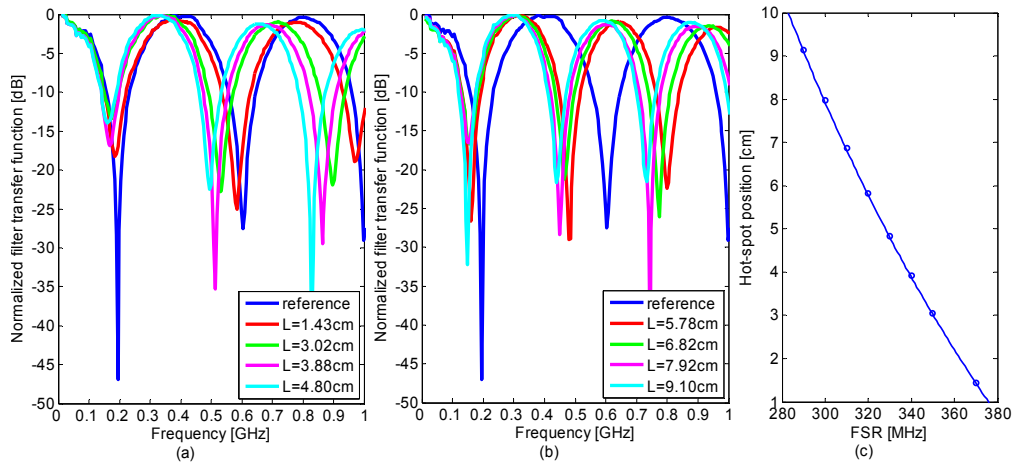


Fig. 6. a) and b) Microwave photonics two tap filters obtained by using a tap provided by a reference arm and a tap provided by a hot-spot located in the long FBG. Insets: position of the hot-spot. Fig. 6. c) Comparison between the hot-spot position calculated from the IFT (dots) and the theoretical inverse linear relation (solid line).

#### 4. Conclusions

In this work, we have proposed and experimentally demonstrated a novel technique for estimating the position and number of hot-spots along a FBG sensor. The measurement system is based on the principle of operation of a MWP filter, in particular on the measurement of the electrical  $S_{21}$  parameter that characterizes the filter transfer function. Two

different alternatives have been proposed in order to estimate the position of a 5 mm hot-spot along the FBG. In the first one, a simple configuration is employed to interrogate a 10-cm long FBG in which the frequency of operation has been swept from 10 MHz to 10 GHz. By evaluating the FSR of the resulting MWP filter, the location of a single hot-spot along the long FBG can be detected with a remarkable accuracy. In the case of two or more hot-spots simultaneously present along the FBG, the fastest method is to derive the corresponding delays by taking the IFT of the measured RF transfer function ( $S_{21}$  parameter). In the second configuration, a reference arm has been used in order to achieve higher time spacing between the taps, which means a shorter FSR. In this case, the hot-spot position has been evaluated by using a less-expensive setup, which includes a modulator and a PD of only 1 GHz bandwidth. In both configurations, the location of the hot-spot in the sensing FBG was calculated with a 0.5 mm spatial accuracy, depending on the instrumental spatial resolution that can be potentially further improved using a higher range instrument. This value simply indicated the potential of the technique in term of accuracy that is certainly attractive in some research areas. For instance, several bio and chemical applications require an accuracy better than 1 mm and in this sense the proposed technique can address and correctly measure local changes in the refractive index over this scale range. Using this simple scheme the magnitude of the hot-spots can also be evaluated by opportunely controlling the tunable bandpass filter, which is a complementary research under study going beyond the scope of this paper.

### **Acknowledgments**

The authors wish to acknowledge the financial support of the Infraestructura FEDER UPVOV08-3E-008, FEDER UPVOV10-3E-492, the Spanish MCINN through the projects TEC2011-29120-C05-05 and TEC2011-29120-C05-01, the Valencia Government through the Ayuda Complementaria ACOMP/2013/146, European Commission through the COST Action TD1001 "OFSeSa" and the Swiss National Science Foundation through project 200021-134546 and the financial support given by the Research Excellency Award Program GVA PROMETEO 2013/012, Next generation Microwave Photonic technologies.